

The Natural History of ‘Oumuamua

The ‘Oumuamua ISSI Team

The discovery of the first interstellar object passing through the Solar System, 1I/2017 U1 (‘Oumuamua), provoked intense and continuing interest from the scientific community and the general public. The faintness of ‘Oumuamua, together with the limited time window within which observations were possible, constrained the information available on its dynamics and physical state. Here we review our knowledge and find that in all cases the observations are consistent with a purely natural origin for ‘Oumuamua. We discuss how the observed characteristics of ‘Oumuamua are explained by our extensive knowledge of natural minor bodies in our Solar System and our current knowledge of the evolution of planetary systems. We highlight several areas requiring further investigation.

1 What we Know about ‘Oumuamua

1I/‘Oumuamua was discovered on 2017 October 19 in the w_{PS1} -band observations of the PanSTARRS1 (PS1) Near Earth Object survey¹. ‘Oumuamua was discovered three days after its closest approach to Earth at 0.16 au, well after it had passed closest to the Sun on 2017 September 9 at a perihelion distance of 0.25 au. By October 22 there was sufficient astrometry to securely identify that the orbit was hyperbolic¹. Because of its rapid motion, there was only a short interval during which observations were possible. Within a week the brightness had dropped by a factor of 10 and within a month by a factor of 100.

The average brightness measured in visible wavelengths during the week after its discovery gave $H_V=22.4^{1,2}$, providing the first indication that ‘Oumuamua has a radius in the hundred-meter range. *Spitzer Space Telescope* observations in the infrared on November 21–22 did not detect ‘Oumuamua³. Their upper limits on the flux imply an effective radius between 49–220 m, depending on the assumed surface properties. For surface scattering parameters (called beaming parameters) that are typical of comets, this implies an effective radius of 70 m and a geometric albedo of 0.1. Relatively few minor bodies this small have been as well characterized physically, which hampers aspects of direct comparison of ‘Oumuamua with similar objects from the Solar System.

Several teams obtained photometric and spectral data in the optical to near-infrared to characterize ‘Oumuamua’s surface composition. ‘Oumuamua is red, similar to many Solar System small bodies, e.g., comets, D-type asteroids, some Jupiter Trojans, and the more neutral trans-Neptunian objects^{1,2,4–7}. Published measurements give a red slope at optical wavelengths of $\sim 10\text{--}20\%/100\text{ nm}$. While the color is consistent with organic-rich surfaces, it is also consistent with iron-rich minerals, and with space weathered surfaces⁸. Thus, color alone is not diagnostic of composition. Comparing the published spectroscopic and photometric data implies that some spectral variability with rotational phase is plausible within the data’s uncertainties, but not certain^{6,9}. As albedo and spectral variability do not necessarily correlate, this does not imply any albedo variation, although it cannot be ruled out.

‘Oumuamua exhibited short-term brightness variation of over a factor of ten (>2.5 magnitudes)^{1,2,5,7,10}. The brightness range was unusually large. Of the minor planets in our Solar System with well-quantified light curves, there are only a handful of asteroids with brightness variations of this scale (¹¹; last updated 31 January 2019). In most cases, these particularly high-amplitude light curves are based on observations of sub-100 m near-Earth asteroids at high phase angles, or on fragmentary light curves of slow-rotating objects.

While brightness variations can be due to variations in the viewing geometry of a particular shape, or due to patchy albedo across a surface, minor planets’ light curves are usually assumed to be shape-dominated, as their surfaces are thought to be covered by small regolith that is evenly distributed across the surface¹². ‘Oumuamua’s light curve shape, with narrow “V-shaped” minima and broad maxima, is indicative that its large brightness variations are caused by its shape, rather than variations in its albedo¹³. Both phase angle and rotation state need to be considered in understanding ‘Oumuamua’s shape. Only a limited range of phase angles ($19\text{--}27^\circ$) could be observed in the short time span during which observations useful for defining ‘Oumuamua’s rotation were made. Accounting for the known effect of the enhancement of amplitude with increasing phase angle¹⁴, the true ratio of longest axis to shortest axis was inferred to be $\geq 6:1$ ¹⁵. Due to the unknown orientation of ‘Oumuamua’s rotation pole, this axial ratio represents only a lower limit.

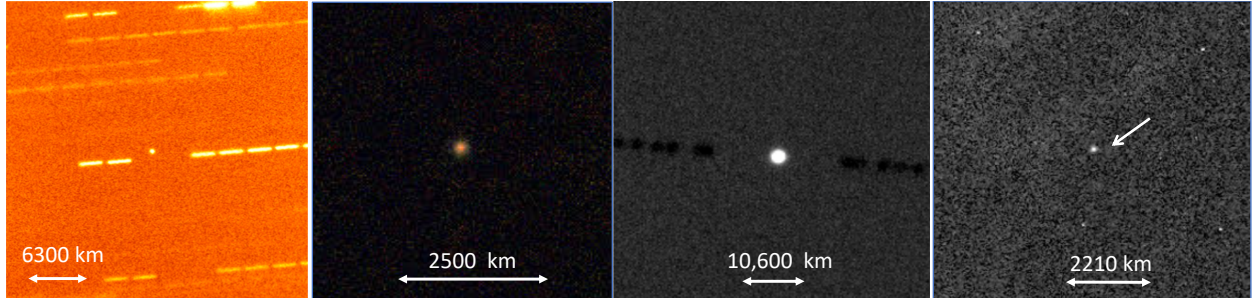


Figure 1: Montage of images of ‘Oumuamua showing its point-like unresolved appearance with no hint of detectable activity. From left to right: 0.4 hr integration through an R-band filter with the Nordic Optical Telescope on 2017 October 26²; “true color” image simulated from *grizY*-band images obtained on 2017 October 27 for a total integration of 1.6 hr with the Gemini South telescope¹; a deep 3.6 hr *r*-band composite image obtained on 2017 October 27-28 with the Gemini North telescope¹⁶; and an F350LP image from *Hubble Space Telescope*¹⁷.

‘Oumuamua’s brightness varied on a timescale of about 4 hours (implying a rotation period of ~ 8 hours for a double-peaked lightcurve), but the various teams did not converge on a consistent rotation period while it was visible. Analysis of the full photometric data set showed that ‘Oumuamua was in a state of excited rotation^{9,16,18}. The most comprehensive model published to date¹⁸ concluded that ‘Oumuamua is rotating around its shortest axis with a period of 8.67 ± 0.34 hours, and has a likely period of rotation around the long axis of 54.48 hours. How we interpret the shape of ‘Oumuamua depends on its specific state of rotation, including its rotation pole. ‘Oumuamua can either have a narrow elongated-ellipsoid shape or a shape more reminiscent of a flattened oval.

Sensitive searches for activity (Fig. 1) showed no evidence for micron-sized dust near ‘Oumuamua^{1,2,4,17}. However, the observations were not sensitive to the detection of millimeter-sized and larger dust, so we have no constraints for the presence of large grains. There was also no detection of any gas, including searches for CN, H₂O, CO and CO₂^{3,4,6,19}, although the level to which each gas can be ruled out varies significantly. We summarize these and other measured properties of ‘Oumuamua in Table 1.

A detailed investigation of the astrometric position measurements from the first observations in mid-October 2017 through the last observations obtained by the *Hubble Space Telescope* on January 2, 2018, showed that a gravity-only orbit provided an inadequate fit to the data. Instead, the data were well fit with the addition of a radial acceleration varying as $1/r^2$, where r is the heliocentric distance¹⁷. This type of acceleration is frequently used in orbital studies of comets, and usually interpreted as being due to an activity-driven cometary acceleration consistent with the decreasing energy with distance from the Sun.

2 A Critical Review of Current Theories

The detection of interstellar objects was anticipated for decades²¹ due to our understanding of how planetary systems form and evolve, but ‘Oumuamua managed to surprise us nonetheless. Most notably, it was generally assumed that the first interstellar object would be an obviously active comet because they are much brighter than an asteroidal object for a given nucleus size. The assumption seemed natural because of the expected similarity between interstellar interlopers and objects from the Solar System’s Oort cloud that have been stored in the deep-freeze of deep-space for billions of years. Since it was thought that most objects from the Oort cloud appear as long period comets, the interstellar objects were expected to have the same morphology. Thus, with limited exceptions²², most speculation on the properties and discovery of interstellar objects involved strongly active comets. The belief that most Oort cloud objects become active comets when they enter the inner solar system drove most of the limits on the spatial density of interstellar objects. We now know that there are many inactive or weakly active Oort cloud objects²³ and if we assume that interstellar objects share the same characteristics then their spatial density would be higher than originally expected. The second surprising aspect of ‘Oumuamua is that it was discovered much faster than expected — early predictions were that PanSTARRS1 was unlikely to detect an interstellar object in 10 years of operation²⁴. Finally, ‘Oumuamua is much

Table 1: A summary of measured properties of ‘Oumuamua

Quantity		Value	References
Dynamical Properties			
Perihelion distance	q [au]	0.255912 ± 0.000007	[1]
Eccentricity	e	1.20113 ± 0.00002	[1]
Incoming radiant	α, δ [deg]	279.4752, 33.8595	[2]
Earth close approach	Δ [au]	0.16175 ± 0.00001	[1]
Incoming velocity	v_∞ [km s ⁻¹]	26.4204 ± 0.0019	[2]
Non-grav acceleration	$A_1 r^{-2}$ [m s ⁻²]	$(4.92 \pm 0.16) \times 10^{-6}$	17
Physical Properties			
Absolute magnitude	H_V	22.4 ± 0.04	1
Albedo	p_V	$> [0.2, 0.1, 0.01]$	3
Effective diameter	D_N [m]	$< [98, 140, 440]$	3
Rotation state		complex, long-axis mode	9, 16, 18
Rotation period	P [hr]	8.67 ± 0.34 hr (long-axis precess)	18
Axis ratio	a:b	$> 6:1$	15
Shape		cigar, or oblate spheroid	18
Spectral slope	S_V [% per 100 nm]	$23 \pm 3, 10 \pm 6, 9.3-17$	1, 4, 6
Surface spectral type		D-type	1, 6
H ₂ O production	$Q(\text{H}_2\text{O})$ [molec s ⁻¹]	4.9×10^{25} @ 1.4 au (model)	17
OH production	$Q(\text{OH})$ [molec s ⁻¹]	$< 1.7 \times 10^{27}$ @ 1.8 au (obs)	19
Hyper volatile (CO?)	$Q(\text{X})$ [molec s ⁻¹]	4.5×10^{25} @ 1.4 au (model)	17
CO ₂ production	$Q(\text{CO}_2)$ [molec s ⁻¹]	$< 9 \times 10^{22}$ @ 2.0 au (obs)	3
CO production	$Q(\text{CO})$ [molec s ⁻¹]	$< 9 \times 10^{23}$ @ 2.0 au (obs)	[3]
CN production	$Q(\text{CN})$ [molec s ⁻¹]	$< 2 \times 10^{22}$ @ 1.4 au (obs)	4
C ₂ production	$Q(\text{C}_2)$ [molec s ⁻¹]	$< 4 \times 10^{22}$ @ 1.4 au (obs)	4
C ₃ production	$Q(\text{C}_3)$ [molec s ⁻¹]	$< 2 \times 10^{21}$ @ 1.4 au (obs)	4
Dust production	$Q(\text{dust})$ [kg s ⁻¹]	$< 1.7 \times 10^{-3}$ @ 1.4 au (obs)	1
		< 10 @ $\sim 10^3$ au (obs)	[3]

[†]Reference Key: [1] JPL Horizons orbital solution #16; [2]²⁰ using the pure $1/r^2$ radial acceleration solution from 17; [3] M. Mommert (priv. comm.) revising the calculation in 3.

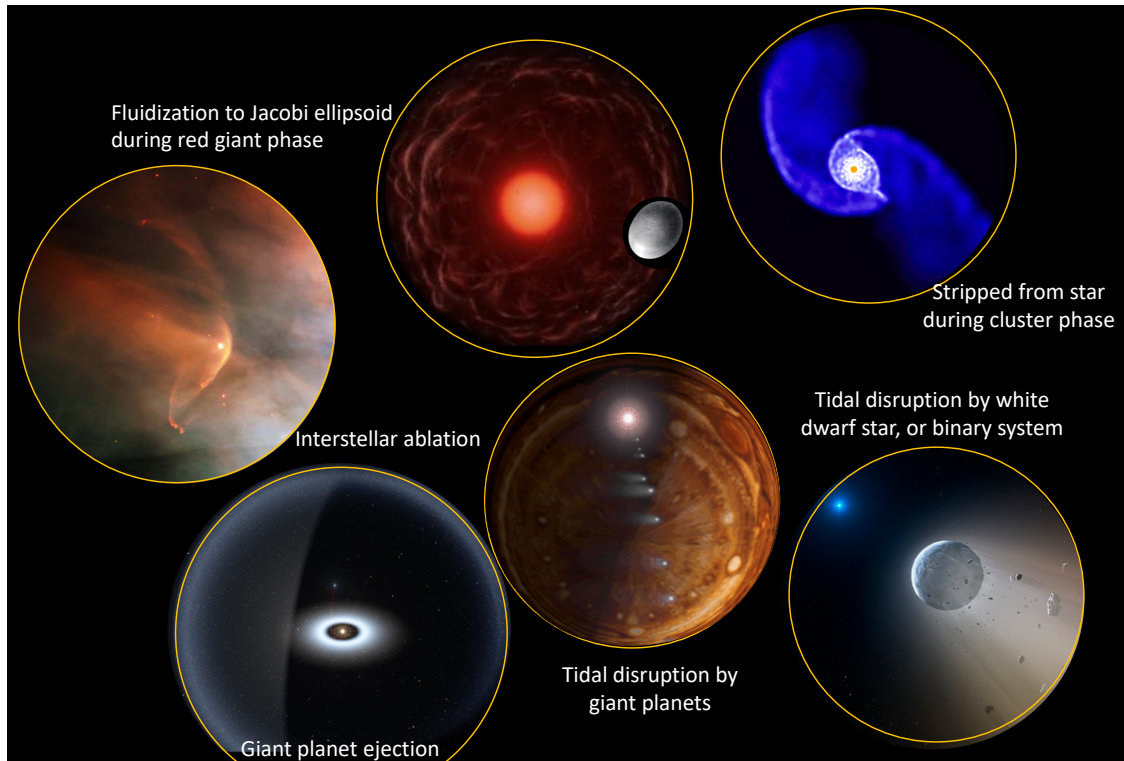


Figure 2: Montage of potential formation scenarios of ‘Oumuamua as a natural planetesimal.

smaller than would have been imagined as the expectation was that it would be similar to a long period comet, a km-scale active object. Detecting and characterizing objects within our own Solar System of ‘Oumuamua’s size is limited to near-Earth objects, so that even if its size had been anticipated there are limited examples from which to form our expectations. Furthermore, even if its small size had been predicted, with a corresponding likelihood of being irregularly shaped, no one would have imagined it to be so unusually elongated. Despite all these surprises ‘Oumuamua’s properties can be readily and naturally explained.

‘Oumuamua Originated in a Planetary System A number of processes have been invoked to explain ‘Oumuamua’s origins and peculiarities since its discovery (Fig. 2). These models generally expect ‘Oumuamua or its parent body to have been born as a planetary building block – a planetesimal – in a gas-dominated protoplanetary disk around a young star. Planetary disks containing planetesimals are common around very young stars (<3 Myr^{25,26}). Roughly 20% of slightly older Sun-like stars are observed to still have mid-infrared excess emission²⁷, interpreted as the dust generated by colliding outer planetesimals (“debris disks”²⁸). This implies that a large fraction of stars are indeed born with large reservoirs of planetesimals capable of being dynamically ejected.

A straightforward explanation for ‘Oumuamua is that it is a planetesimal (or a planetesimal fragment) ejected from its home system^{29,30}. During planetary system formation, a significant portion of a system’s planetesimals are ejected into interstellar space³¹. Gravitational interactions with the stars of the surrounding cluster or with the giant planets of the planetary system itself are major mechanisms of ejection³². Simulations show that planetesimals are most efficiently ejected in systems in which the giant planets themselves become unstable³³. In close binary systems (with a planet-forming disk exterior to two stars), planetesimals that enter within a critical distance to the binary are destabilized³⁴ and quickly ejected as interstellar objects³⁵. Close stellar flybys, which are common during the $\sim 3 - 5$ Myr-long embedded cluster phase³⁶, can strip planetesimals from the outer parts of planetary systems³⁷. As their host stars evolve off the main sequence and lose mass, planetesimals will eventually also be liberated from their home systems³⁸.

The Expected Number Density of Interstellar Objects in Space Combining the observed absolute magnitude of ‘Oumuamua with current sky-survey detection limits, the number density of objects in interstellar space of the same size as ‘Oumuamua or larger is about 0.1 per cubic au^{1,39,40}. This estimate applies to objects with little to no activity (like ‘Oumuamua) and implies that interstellar objects are continuously passing through the Solar System below our current detection threshold.

It has been asserted that this number density of interstellar objects is 2–8 orders of magnitude higher than would be expected from planet formation scenarios⁴¹. However, transforming a number density of interstellar objects to a mass density requires a knowledge of the population’s size–frequency distribution (SFD)⁴². With a single detected object there are no firm constraints on this distribution: until the interstellar object SFD is known from tens of detections, there is a disconnect between the measured number density of interstellar objects and their mass density.

We show with a simple experiment that the expected number density of interstellar objects varies by many orders of magnitude depending on the SFD applied to the mass (Fig. 3). Our estimate is based on the idea that ‘Oumuamua is a planetesimal (or a planetesimal fragment) that was ejected from its home system by giant planets^{29,33}.

We first estimate the underlying mass density of interstellar objects based on planet formation theory and observational constraints. The density and mass distribution of stars are well-known⁴³; they are dominated by low-mass stars, with a Galactic disk-averaged value of ~ 0.2 stars per cubic parsec. Virtually all stars host planets⁴⁴. Radial velocity surveys find that ~ 10 – 20% of Sun-like stars have gas giants⁴⁵ but this fraction drops significantly for low-mass stars⁴⁶. The stellar mass-averaged frequency of gas giants is ~ 1 – 10% ⁴⁷. Microlensing surveys find that the occurrence rate of ice giants is significantly higher (~ 10 – 50%) and has a weaker stellar mass dependence⁴⁸. Similarly, the ubiquity of gap structures in the ALMA disks suggests that Neptune-mass planets are common at large distances, with an occurrence rate estimated at $\sim 50\%$ ⁴⁹.

How much mass in planetesimals does each system eject? This depends on the dynamics of each individual system and whether the planets remain stable³³. We assume that each gas giant system ejects 1–100 Earth masses³³. The abundant ice giants also efficiently eject planetesimals during⁵⁰ and after³² their formation; we assume each ice giant system ejects 0.1–10 Earth masses. Allowing for the frequency of the types of planetary systems, this comprises 0.1–10 Earth masses per star ejected by gas giants and 0.01–5 Earth masses by ice giants. This totals 0.02 to 15 Earth masses in interstellar objects per star or 0.004 to 3 Earth masses per cubic parsec.

We then calculate the expected number density of interstellar objects from that mass density estimate. Figure 3 shows the huge diversity of number densities of interstellar objects that can be inferred: the differences arise purely from the choice of plausible size–frequency distribution. While the uncertainty in our estimate of ejected planetesimal mass per star spans three orders of magnitude, the difference in inferred number density between SFDs is even larger. For example, a power-law distribution characteristic of planetesimal formation simulations (SFD a_1) requires an implausibly large amount of mass – thousands of Earth masses – to be ejected per star in order to match the observational constraint on the number density^{29,51–53}. However, several SFDs from Fig. 3 with somewhat more mass in small objects (e.g., SFD b_2 has 3% by mass in fragments and is otherwise similar to SFD a_1) can match the measured interstellar object number density. It is easier to match the inferred number density at the higher end of our estimate of the interstellar object mass density, but the main uncertainty comes from the assumed SFD.

Thus, given that the number density of interstellar objects cannot yet be reliably related to the mass density, the claim that the observed number density is presently “higher than expected” from planet formation scenarios is not supported.

Uniqueness of the Trajectory While not typical for field stars, ‘Oumuamua’s trajectory is exactly what was expected for detectable interstellar objects²². As they age, stars in the solar neighbourhood are perturbed away from the Local Standard of Rest, which is defined by the galactic motions of nearby stars. Of course, a small fraction of older stars may still have small random velocities⁵⁸. ‘Oumuamua’s random velocity is 9 km s^{-1} from the Local Standard of Rest, far smaller than the $\sim 50 \text{ km s}^{-1}$ velocity dispersion of nearby stars⁵⁹. This small random velocity could imply that ‘Oumuamua is dynamically young¹, with a statistically-derived dynamical age of $< 2 \text{ Gyr}$ ^{60,61}.

Gravitational focusing by the Sun creates an observational bias that favors the detection of interstellar objects with low random velocities, like that of ‘Oumuamua²². This means it is challenging to use ‘Oumuamua’s galactic motion

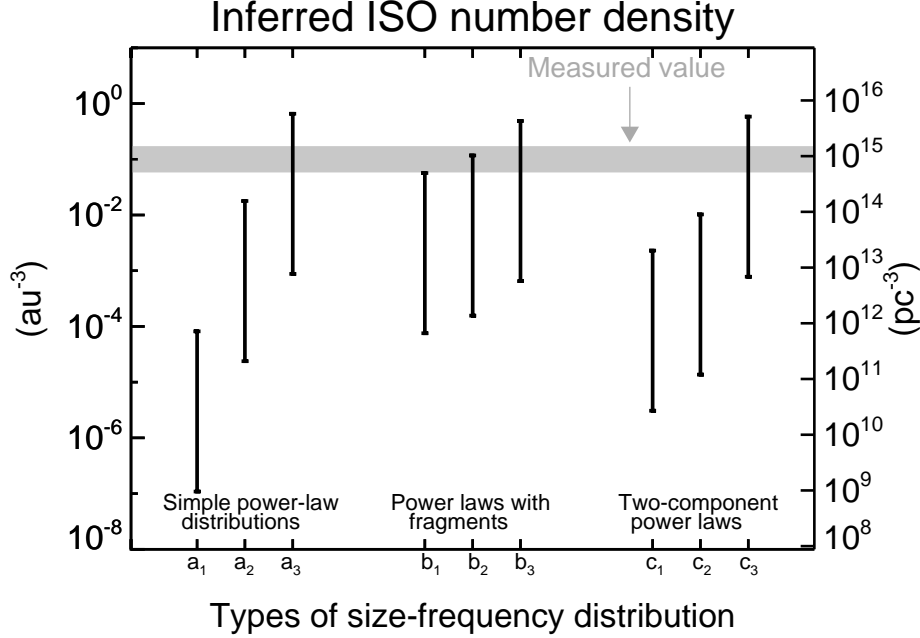


Figure 3: Inferred number density of interstellar objects – for a fixed estimate of the mass density of 0.004–3 Earth masses per cubic parsec – assuming different underlying size-frequency distributions (SFDs). We tested three SFDs: 1) power laws (a_{1-3}) in which the number of objects N of a given mass m is $N(m) \propto m^{-x}$; 2) power laws in which a small fraction (typically 1%) of the mass has been converted into fragments – comparable in size to ‘Oumuamua, perhaps due to tidal disruption from giant planet encounters prior to ejection^{29,30} (b_{1-3}); and 3) two-component power laws (c_{1-3}). The power laws extend from effective radii r_{min} to r_{max} with $N(m) \propto m^{-x}$, and all three have $r_{max} = 100$ km. Distribution a_1 is consistent with simulations of planetesimal formation^{54,55} and has $r_{min} = 100$ m and $x = 0.6$. Distribution a_2 assumes collisional equilibrium⁵⁶ and has $r_{min} = 50$ m and $x = 5/6$. Distribution a_3 is bottom-heavy (the smallest objects dominate by mass); it extrapolates the size-frequency distribution of boulders on comet 67P/Churyumov-Gerasimenko⁵⁷ to large sizes and has $r_{min} = 50$ m and $x = 1.2$. Distribution b_1 contains 99% of its mass following distribution a_2 with 1% by mass in 50 m-sized fragments. Distribution b_2 contains 97% of its mass following distribution a_1 and 3% in 50 m-sized fragments (see ²⁹). Distribution b_3 is a single-size distribution, assuming that all interstellar objects are ‘Oumuamua-sized (100 m). Distributions c_1 through c_3 all assume $r_{min} = 50$ m and $r_{max} = 100$ km. Distribution c_1 has $x = 0.6$ for objects larger than $r_{break} = 1$ km and $x = 5/6$ for smaller ones. Distribution c_2 has the same power laws but with $r_{break} = 10$ km. Distribution c_3 has $x = 0.6$ for objects larger than $r_{break} = 10$ km and $x = 1.2$ for smaller ones.

to constrain the interstellar object population’s velocity dispersion. Indeed, as demonstrated in Figure 4, there appears to be nothing unusual about the specific parameters of ‘Oumuamua’s hyperbolic trajectory, as its perihelion distance, eccentricity, and inclination agree well with the predicted distribution of the values for interstellar objects detectable by the major contemporary asteroid surveys — a prediction published²² nearly eight months *before* ‘Oumuamua was discovered!

“Cometary” Activity and Retention of Volatile Materials The mass loss needed to explain ‘Oumuamua’s observed non-gravitational acceleration¹⁷ is on the order of 1 kg s^{-1} . Outgassing models for an object the size of ‘Oumuamua with comet-like properties can produce this amount of mass loss at the distances observed⁶². Furthermore, when the *Rosetta* observations of comet 67P/Churyumov-Gerasimenko (made at comparable heliocentric distances to when ‘Oumuamua was observed) are scaled down to an ‘Oumuamua-sized object, they yield a similar outgassing rate⁶³. Depending on the assumptions, the total mass lost during the interval of observations may represent up to $\sim 10\%$ of

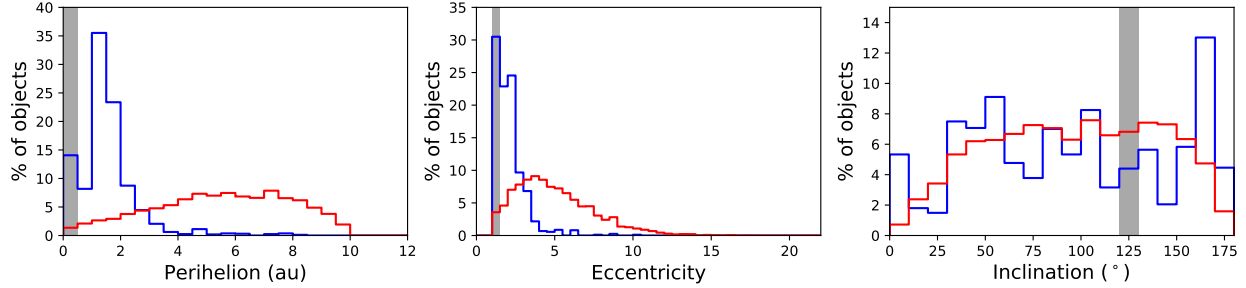


Figure 4: Predicted distribution of orbital elements of natural interstellar objects (blue curves are inactive objects, red curves are active objects) detected by the primary contemporary asteroid surveys (adapted from ²²). In each distribution, ‘Oumuamua (gray vertical bar) has orbital elements at or near the most likely orbital elements for inactive objects.

‘Oumuamua’s total mass⁶⁴.

A typical comet with this level of outgassing would produce dust of all sizes, yet no dust was detected. The absence of a radiation-pressure-swept tail indicates that if any particles were released, the effective particle size must be large. Observations by both ground-based telescopes and space missions to comets have shown that the ejection of fine-grained dust, which dominates the reflected light at visible wavelengths, is not always correlated with gas release. For example, comet 2P/Encke reaches a similar perihelion distance as ‘Oumuamua, and it often lacks any detectable dust at visible wavelengths⁶⁵. Some long-period comets preferentially eject large particles due to a mechanism that is currently not understood⁶⁶. Unfortunately, no observations were sensitive to large dust grains, which are most detectable in radio wavelengths, and meteor observations (sensitive to 0.1–1 mm dust) can only rule out activity at unrealistically large heliocentric distances (> 1000 au) or with unusual strength⁴.

The search for gas emission from ‘Oumuamua was not comprehensive owing to the challenging observing circumstances. There were no observations that could have made sensitive enough detections of water outgassing to test for comet-like activity. The relative abundance of CN to H₂O of ‘Oumuamua needed to reconcile the non-detections of CN⁴ with the inferred H₂O outgassing rate needed to account for non-gravitational forces¹⁷, while unusual, is not unprecedented. ‘Oumuamua needed to be depleted in CN by at least a factor of 15 relative to typical abundances in comets, while comets C/1988 Y1 Yanaka⁶⁷ and 96P/Machholz 1⁶⁸ were depleted by factors of 25 and 72, respectively. One of these highly depleted comets, 96P, also has a very low amount of dust observed at visible wavelengths compared to gas⁶⁸, like ‘Oumuamua.

The upper limits to the CO and CO₂ production rates³ (and M. Mommert priv. comm.) combined with the inferred H₂O production rate imply abundances of CO/H₂O $\leq 2\%$ and CO₂/H₂O $\leq 0.2\%$. This CO upper limit is within the range of measurements for known comets, while the CO₂ upper limit is about an order of magnitude lower⁶⁹. However, CO₂ is difficult to measure, so the known sample may be biased to higher abundances. Both CO and CO₂ are much more volatile than H₂O, resulting in a trend to lower ratios with smaller heliocentric distances⁷⁰. The volatility difference would have resulted in CO and CO₂ being depleted deeper than H₂O. Thus, ‘Oumuamua may have lost most/all of its CO and CO₂ prior to the observations that would have constrained their abundances. Alternatively, it may have had intrinsically low abundances of CO and CO₂ due to formation conditions in its home system. The range of these ratios of volatiles in comets has recently been found to be far greater than was previously known: C/2016 R2 PanSTARRS has CO/H₂O at least several orders of magnitude higher than any other measured comet, with no H₂O yet conclusively detected⁷¹.

Thermal models show that ices may exist within just ~ 30 cm of the surface without being released during ‘Oumuamua’s perihelion passage^{6,72}. A natural consequence would be a thermal lag in which outgassing begins significantly later. Such a scenario would decrease the total amount of volatile material needed to explain the observed non-gravitational acceleration and shorten the timescale over which torques were at work. One thermal model was shown

to be consistent with the observed non-gravitational acceleration by assuming outgassing from water in combination with another volatile species¹⁷.

Based on the lack of detected activity, it has been suggested that ‘Oumuamua had repeated passages close to its host star before being ejected³⁰. Such repeated close passages can remove volatiles from planetesimals’ surfaces and render ejected planetesimals inactive, or extinct⁷³. Models that match the various distributions of Solar System comets⁷⁴ predict that smaller objects become inactive more quickly, so it could simply be that 100-m scale ejected objects like ‘Oumuamua are devolatilized in their outer layers. There could very well be a population of inactive small objects from our own Oort cloud that goes undetected because of their lack of activity, as evidenced by the Manx objects²³.

Besides outgassing, a number of possible explanations for the observed non-gravitational acceleration were considered, but ultimately rejected¹⁷. Most prominently was solar radiation pressure, which required ‘Oumuamua’s density to be 3–4 orders of magnitude lower than that of asteroids of similar size (solar radiation pressure effects have been detected on a few small asteroids⁷⁵). Alternate explanations in support of solar radiation pressure have suggested that ‘Oumuamua had a low density due to a fractal aggregate structure produced either by devolatilization of a comet-like body prior to its discovery⁷⁶ or having formed as a very large aggregate of icy dust particles beyond the snow line in its home system⁷⁷. Such extended, extremely low density objects have never been detected, but might naturally explain some other phenomena observed for disrupting comets⁷⁶ or help reconcile some aspects of protoplanetary disc models⁷⁷.

Alien technology? The idea of ‘Oumuamua as alien technology has been advocated in a series of papers^{41,78,79}. The authors argue that the dimensions needed to explain the observed solar radiation pressure are consistent with a “solar sail.” While this fits some aspects of the observations — the basic idea of ‘Oumuamua having a highly flattened shape was previously considered^{17,18} — it appears unable to explain other key aspects of the observations, and some arguments in favor of this hypothesis are simply wrong.

The key argument against the solar sail hypothesis is ‘Oumuamua’s light curve amplitude. In order for a solar sail to cause the observed non-gravitational acceleration, it needs to remain properly oriented towards the Sun. However, in order to yield the observed brightness variations, its orientation would need to be varying as viewed from Earth. Furthermore, since the actual dimensions of the solar sail would be $> 10 : 1$, the orientation as viewed from Earth would need to be very nearly edge on, and remain so throughout the observations despite viewing geometry changes. It has not been shown that an orientation exists that can achieve all of these constraints imposed by the observational data. Furthermore, as discussed earlier, the shape of ‘Oumuamua’s light curve, with broad maxima and narrow minima, is consistent with an elongated ellipsoid.

The claim⁷⁸ that ‘Oumuamua must be at least ten times “shinier” than all Solar System asteroids to make the *Spitzer Space Telescope* data consistent with the ground based observations is incorrect. The *Spitzer* observations are consistent with geometric albedos $0.01 \leq p_v \leq 0.5^3$, with a most likely albedo of $p_v \sim 0.1$. Comets have geometric albedos of $p_v = 0.02 - 0.07$, carbonaceous and silicate asteroids have $p_v = 0.05 - 0.21$, and the most reflective asteroids have $p_v \sim 0.5^{80,81}$. Thus ‘Oumuamua’s measured reflectivity of ~ 0.1 is entirely consistent with normal Solar System small bodies.

Finally, it was argued that ‘Oumuamua was deliberately sent toward Earth based on its “unusual” kinematics and presumed scarcity⁴¹. While provocative, this argument is baseless. First, ‘Oumuamua’s trajectory is consistent with predictions²² for detectable inactive interstellar objects. Second, the measured number density cannot be claimed to be at odds with expectations because of our ignorance of the size distribution of interstellar objects.

Thus, we find no compelling evidence to favor an alien explanation for ‘Oumuamua.

3 Open questions

We have discussed the many aspects of ‘Oumuamua’s properties that can be explained naturally. However, there remain several unanswered questions regarding ‘Oumuamua that warrant further study.

Shape While several models have been proposed to explain ‘Oumuamua’s very elongated shape, none can naturally match such an extreme axis ratio (of at least 6:1) within a self-consistent framework. One model⁸² invokes the complete

fluidization of a planetesimal by an evolving red giant star, causing the object to assume the shape of a high angular momentum Jacobi ellipsoid. Other models have proposed that ‘Oumuamua is a fragment of a planetesimal^{30,76,83} or planet⁸⁴ that was tidally disrupted after a very close passage to a low-mass star, white dwarf, or giant planet, or simply as it neared perihelion. It remains to be demonstrated whether such disruption events create fragments as stretched-out as ‘Oumuamua appears to be. A third model proposes that a large number of high-velocity impacts with dust grains may create sharp edges and planar surfaces on small bodies⁸⁵ or simply erode enough material to substantially increase the axis ratio of small objects⁸⁶, while a fourth proposes that it formed from a low speed collision between two ~ 50 m planetesimals in a protoplanetary disk⁸⁷. In the context of these models, it remains to be understood why such extreme shapes are so rare among larger Solar System bodies; though this may partly be an observational selection effect. At two orders of magnitude larger than ‘Oumuamua, the primordial Kuiper belt object 2014 MU₆₉ has a bi-lobed structure with substantive “pancake” flattening to the larger lobe⁸⁸.

Rotation state The ensemble of published photometry reveals that ‘Oumuamua is in non-principal axis rotation (NPA)^{9,16,18}, which is a spin state commonly observed among asteroids, including objects as small as ‘Oumuamua⁸⁹. The details of the NPA are non-unique from the available data, including when ‘Oumuamua achieved NPA rotation. Disruption or strong gravitational encounters could have created the NPA state, and the $> 10^{11}$ yr damping timescale is sufficiently long that the tumbling may have originated in or during departure from its home system^{9,16,18,90}. Alternatively, the NPA rotation might have occurred during ‘Oumuamua’s journey through our system. It has been argued that the level of outgassing needed to explain the non-gravitational acceleration would have resulted in a rapid change in rotation period⁸³. Even a small asymmetry in the torquing might have perturbed ‘Oumuamua from simple rotation to NPA rotation.

One work found that if the large non-gravitational acceleration was caused by typical cometary outgassing, then the associated torques should have caused ‘Oumuamua to rapidly spin up beyond its rotational break up limit⁸³. In contrast, others showed that outgassing activity that followed the subsolar point of an elongated body could produce the observed non-gravitational acceleration and would naturally result in NPA rotation with a lightcurve amplitude and period comparable to the observations, without causing extreme spin up⁶⁴.

The orientation of ‘Oumuamua’s rotational angular momentum vector is unconstrained from the finite available data, but is critical for properly assessing the shape from the light curve. Dynamical work found that the rotation can be in one of five different modes, and if it is closest to its lowest rotational energy the shape can resemble the elongated “cigar-like” shape, and only in the highest energy state would it be an “extremely oblate spheroid”¹⁸. The “cigar-like” shape is the more likely configuration, both because it is energetically more stable and because it permits a much larger range of orientations on the sky (as previously discussed, a very flat shape requires a very specific orientation to produce the observed light curve).

Home system In spite of many attempts to trace the orbit of ‘Oumuamua back to its home system^{20,91–93} or star cluster^{94,95}, no convincing candidate origin star systems or stellar associations have been identified. Whether tracing back to a unique origin is feasible depends on how long ago ‘Oumuamua was ejected from its home system, since more distant regions must be considered for longer travel times, and whether it had past encounters, since each effectively erases its dynamical past. Although future data releases of high precision surveys like Gaia are likely to spur deeper searches and may yet reveal plausible candidates, it is likely that no system will be definitively shown to be ‘Oumuamua’s origin.

In addition to travel time, uncertainties in velocity/acceleration affect our ability to identify its home system. The first generation of searches^{91–95} were based on the Keplerian orbit solution available at the time, while a later study²⁰ utilized the solution that included non-gravitational acceleration, assuming that it was symmetric pre- and post-perihelion. Whether this assumption is justified is ultimately unknown as no pre-perihelion observations are available, but it is likely that outgassing was delayed due to a thermal lag⁶. Without observational constraints, the parameter space to search for a home system increases considerably.

4 Conclusions

As the first interstellar visitor to our solar system, ‘Oumuamua has challenged many of our assumptions about how small bodies from another star system would look. While ‘Oumuamua presents a number of compelling questions, we have shown that each can be answered by assuming ‘Oumuamua to be a natural object. Assertions that ‘Oumuamua may be artificial are not justified when the wide body of current knowledge about solar system minor bodies and planetary formation is considered.

The Large Synoptic Survey Telescope (LSST) is expected to begin full operations in 2022 and is predicted to discover on the order of one interstellar object per year^{39,72,96}. Thus, we will soon have a much better understanding of how common — or rare — the properties of ‘Oumuamua are. This knowledge will yield great insight into the planetesimal formation, evolution, and ejection processes at work across the Galaxy.

THE ‘OUMUAMUA ISSI TEAM:

Michele T. Bannister (Astrophysics Research Centre, Queen’s University Belfast, Belfast BT7 1NN, UK) [ORCID: 0000-0003-3257-4490]

Asmita Bhandare (Max-Planck-Institut für Astronomie, Königstuhl 17, 69117 Heidelberg, Germany)[ORCID: 0000-0002-1197-3946]

Piotr A. Dybczyński (Astronomical Observatory Institute, Faculty of Physics, A. Mickiewicz University, Słoneczna 36, Poznań, Poland) [ORCID: 0000-0003-1492-4602]

Alan Fitzsimmons (Astrophysics Research Centre, Queen’s University Belfast, Belfast BT7 1NN, UK) [ORCID: 0000-0003-0250-9911]

Aurélie Guilbert-Lepoutre (Institut UTINAM, UMR 6213 / CNRS and Université de Bourgogne-Franche Comté, F-25000 Besancon, France; Laboratoire de Géologie de Lyon, LGL-TPE, UMR 5276 CNRS / Université de Lyon / Université Claude Bernard Lyon 1 / ENS Lyon, 69622 Villeurbanne, France) [ORCID: 0000-0003-2354-0766]

Robert Jedicke (Institute for Astronomy, University of Hawaii, 2680 Woodlawn Drive, Honolulu, HI 96822, USA) [ORCID: 0000-0001-7830-028X]

Matthew M. Knight* (University of Maryland, Department of Astronomy, College Park, MD 20742, USA) [ORCID: 0000-0003-2781-6897]

Karen J. Meech (Institute for Astronomy, University of Hawaii, 2680 Woodlawn Drive, Honolulu, HI 96822, USA) [ORCID: 0000-0002-2058-5670]

Andrew McNeill (Department of Physics and Astronomy, Northern Arizona University, Flagstaff, AZ 86011, USA)

Susanne Pfalzner (Max-Planck-Institut für Radioastronomie, Auf dem Hügel 69, 53121 Bonn, Germany; Jülich Supercomputing Center, Forschungszentrum Jülich, 52428 Jülich, Germany; Department of Physics, University of Cologne, Zÿpicher Str. 77, 50937 Cologne, Germany) [ORCID: 0000-0002-5003-4714]

Sean N. Raymond (Laboratoire d’Astrophysique de Bordeaux, CNRS and Université de Bordeaux, Allée Geoffroy St. Hilaire, F-33165 Pessac, France) [ORCID: 0000-0001-8974-0758]

Colin Snodgrass (Institute for Astronomy, University of Edinburgh, Royal Observatory, Edinburgh EH9 3HJ, UK) [ORCID: 0000-0001-9328-2905]

David E. Trilling (Department of Physics and Astronomy, Northern Arizona University, Flagstaff, AZ 86011 USA) [ORCID: 0000-0003-4580-3790]

Quanzhi Ye (Division of Physics, Mathematics and Astronomy, California Institute of Technology, Pasadena, CA 91125, USA; Infrared Processing and Analysis Center, California Institute of Technology, Pasadena, CA 91125, USA) [ORCID: 0000-0002-4838-7676]

*Contacting author: mknight2@umd.edu

DATA AVAILABILITY

The authors declare that the main data supporting the findings of this study are available within the article and its Supplementary Information files. Extra data are available from the corresponding author upon request.

ACKNOWLEDGEMENTS

We thank the International Space Science Institute (ISSI Bern), which made this collaboration possible. AF, MB and CS acknowledge support from UK Science and Technology Facilities Council grants ST/P0003094/1 and ST/L004569/1.

KJM acknowledges support through NSF awards AST1617015, in addition to support for HST programs GO/DD-15405 and -15447 provided by NASA through a grant from the Space Telescope Science Institute, which is operated by the Association of Universities for Research in Astronomy under NASA contract NAS 5-26555. QY is supported by the GROWTH project funded by the National Science Foundation under Grant No. 1545949. This research was partially supported by the project 2015/17/B/ST9/01790 funded by the National Science Centre in Poland. MMK acknowledges support from NASA Near Earth Object Observations grant #NNX17AK15G. AGL acknowledges funding from the European Research Council (ERC) under grant agreement No 802699. AM and DET are supported in part by Spitzer/NASA through an award issued by JPL/Caltech. SNR acknowledges helpful discussions with Phil Armitage related to the interstellar object number/mass density, and the Virtual Planetary Laboratory research team, funded by the NASA Astrobiology Program under NASA Grant Number 80NSSC18K0829. This work benefited from participation in the NASA Nexus for Exoplanet Systems Science research coordination network.

AUTHOR CONTRIBUTIONS

MMK and AF organized the ISSI team. KJM created Figures 1 & 2, SNR conducted the modelling of inferred interstellar object number density and created Figure 3. MMK, AF, and RJ created Figure 4 from source data provided by T. Engelhardt. All authors discussed the topics in the paper, contributed to the writing, and commented on the manuscript at all stages.

COMPETING INTERESTS

The authors declare no competing financial interests.

REFERENCES

1. Meech, K. J. *et al.* A brief visit from a red and extremely elongated interstellar asteroid. *Nature* **552**, 378–381 (2017).
2. Jewitt, D. *et al.* Interstellar Interloper 1I/2017 U1: Observations from the NOT and WIYN Telescopes. *Astrophys. J.* **850**, L36 (2017).
3. Trilling, D. E. *et al.* Spitzer Observations of Interstellar Object 1I/‘Oumuamua. *Astron. J.* **156**, 261 (2018).
4. Ye, Q.-Z., Zhang, Q., Kelley, M. S. P. & Brown, P. G. 1I/2017 U1 (‘Oumuamua) is Hot: Imaging, Spectroscopy, and Search of Meteor Activity. *Astrophys. J. Lett.* **851**, L5 (2017). 1711.02320.
5. Bannister, M. T. *et al.* Col-OSSOS: Colors of the Interstellar Planetesimal 1I/‘Oumuamua. *Astrophys. J.* **851**, L38 (2017).
6. Fitzsimmons, A. *et al.* Spectroscopy and thermal modelling of the first interstellar object 1I/2017 U1 ‘Oumuamua. *Nature Astronomy* **2**, 133–137 (2018). 1712.06552.
7. Bolin, B. T. *et al.* APO Time-resolved Color Photometry of Highly Elongated Interstellar Object 1I/‘Oumuamua. *Astrophys. J. Lett.* **852**, L2 (2018). 1711.04927.
8. Moretti, P. F., Maras, A. & Folco, L. Space weathering, reddening and gardening of asteroids: A complex problem. *Advances in Space Research* **40**, 258–261 (2007).
9. Fraser, W. C. *et al.* The tumbling rotational state of 1I/‘Oumuamua. *Nature Astronomy* **2**, 383–386 (2018).
10. Knight, M. M. *et al.* On the Rotation Period and Shape of the Hyperbolic Asteroid 1I/‘Oumuamua (2017 U1) from Its Lightcurve. *Astrophys. J. Lett.* **851**, L31 (2017). 1711.01402.
11. Warner, B. D., Harris, A. W. & Pravec, P. The asteroid lightcurve database. *Icarus* **202**, 134–146 (2009).
12. Fujiwara, A. *et al.* The Rubble-Pile Asteroid Itokawa as Observed by Hayabusa. *Science* **312**, 1330–1334 (2006).

13. Lacerda, P. & Jewitt, D. C. Densities of Solar System Objects from Their Rotational Light Curves. *Astron. J.* **133**, 1393 (2007). astro-ph/0612237.
14. Zappala, V., Cellino, A., Barucci, A. M., Fulchignoni, M. & Lupishko, D. F. An analysis of the amplitude-phase relationship among asteroids. *Astron. Astrophys.* **231**, 548–560 (1990).
15. McNeill, A., Trilling, D. E. & Mommert, M. Constraints on the Density and Internal Strength of 1I/‘Oumuamua. *Astrophys. J. Lett.* **857**, L1 (2018). 1803.09864.
16. Drahus, M. et al. Tumbling motion of 1I/‘Oumuamua and its implications for the body’s distant past. *Nature Astronomy* **2**, 407–412 (2018).
17. Micheli, M. et al. Non-gravitational acceleration in the trajectory of 1I/2017 U1 (‘Oumuamua). *Nature* **559**, 223–226 (2018).
18. Belton, M. J. S. et al. The Excited Spin State of 1I/2017 U1 ‘Oumuamua. *Astrophys. J. Lett.* **856**, L21 (2018). 1804.03471.
19. Park, R. S., Pisano, D. J., Lazio, T. J. W., Chodas, P. W. & Naidu, S. P. Search for OH 18 cm Radio Emission from 1I/2017 U1 with the Green Bank Telescope. *Astron. J.* **155**, 185 (2018). 1803.10187.
20. Bailer-Jones, C. A. L. et al. Plausible Home Stars of the Interstellar Object ‘Oumuamua Found in Gaia DR2. *Astron. J.* **156**, 205 (2018). 1809.09009.
21. McGlynn, T. A. & Chapman, R. D. On the nondetection of extrasolar comets. *Astrophys. J. Lett.* **346**, L105–L108 (1989).
22. Engelhardt, T. et al. An Observational Upper Limit on the Interstellar Number Density of Asteroids and Comets. *Astron. J.* **153**, 133 (2017). 1702.02237.
23. Meech, K. J. et al. Inner solar system material discovered in the Oort cloud. *Science Advances* **2**, e1600038 (2016).
24. Jewitt, D. Project Pan-STARRS and the Outer Solar System. *Earth Moon and Planets* **92**, 465–476 (2003).
25. Haisch, J., Karl E., Lada, E. A. & Lada, C. J. Disk Frequencies and Lifetimes in Young Clusters. *Astrophys. J.* **553**, L153–L156 (2001). astro-ph/0104347.
26. Pfalzner, S., Steinhausen, M. & Menten, K. Short Dissipation Times of Proto-planetary Disks: An Artifact of Selection Effects? *Astrophys. J.* **793**, L34 (2014). 1409.0978.
27. Montesinos, B. et al. Incidence of debris discs around FGK stars in the solar neighbourhood. *Astron. Astrophys.* **593**, A51 (2016). 1605.05837.
28. Wyatt, M. C. Evolution of Debris Disks. *Annu. Rev. Astron. Astrophys.* **46**, 339–383 (2008).
29. Raymond, S. N., Armitage, P. J., Veras, D., Quintana, E. V. & Barclay, T. Implications of the interstellar object 1I/‘Oumuamua for planetary dynamics and planetesimal formation. *Mon. Not. Roy. Astron. Soc.* **476**, 3031–3038 (2018). 1711.09599.
30. Raymond, S. N., Armitage, P. J. & Veras, D. Interstellar Object ‘Oumuamua as an Extinct Fragment of an Ejected Cometary Planetesimal. *Astrophys. J. Lett.* **856**, L7 (2018). 1803.02840.
31. Charnoz, S. & Morbidelli, A. Coupling dynamical and collisional evolution of small bodies: an application to the early ejection of planetesimals from the Jupiter-Saturn region. *Icarus* **166**, 141–156 (2003).
32. Tremaine, S. The distribution of comets around stars. In Phillips, J. A., Thorsett, S. E. & Kulkarni, S. R. (eds.) *Planets Around Pulsars*, vol. 36, 335–344 (1993).

33. Raymond, S. N., Armitage, P. J. & Gorelick, N. Planet-Planet Scattering in Planetesimal Disks. II. Predictions for Outer Extrasolar Planetary Systems. *Astrophys. J.* **711**, 772–795 (2010). 1001.3409.
34. Holman, M. J. & Wiegert, P. A. Long-Term Stability of Planets in Binary Systems. *Astron. J.* **117**, 621–628 (1999). astro-ph/9809315.
35. Jackson, A. P., Tamayo, D., Hammond, N., Ali-Dib, M. & Rein, H. Ejection of rocky and icy material from binary star systems: implications for the origin and composition of 1I/‘Oumuamua. *Mon. Not. Roy. Astron. Soc.* **478**, L49–L53 (2018). 1712.04435.
36. Vincke, K. & Pfalzner, S. Cluster Dynamics Largely Shapes Protoplanetary Disk Sizes. *Astrophys. J.* **828**, 48 (2016).
37. Hands, T. O., Dehnen, W., Gration, A., Stadel, J. & Moore, B. The fate of planetesimal discs in young open clusters: implications for 1I/‘Oumuamua, the Kuiper belt, the Oort cloud and more. *arXiv e-prints* (2019). 1901.02465.
38. Veras, D. Post-main-sequence planetary system evolution. *Royal Society Open Science* **3**, 150571 (2016). 1601.05419.
39. Trilling, D. E. et al. Implications for Planetary System Formation from Interstellar Object 1I/2017 U1 (‘Oumuamua). *Astrophys. J. Lett.* **850**, L38 (2017). 1711.01344.
40. Do, A., Tucker, M. A. & Tonry, J. Interstellar Interlopers: Number Density and Origin of ‘Oumuamua-like Objects. *Astrophys. J. Lett.* **855**, L10 (2018). 1801.02821.
41. Bialy, S. & Loeb, A. Could Solar Radiation Pressure Explain ‘Oumuamua’s Peculiar Acceleration? *Astrophys. J.* **868**, L1 (2018).
42. Moro-Martín, A., Turner, E. L. & Loeb, A. Will the Large Synoptic Survey Telescope Detect Extra-Solar Planetesimals Entering the Solar System? *Astrophys. J.* **704**, 733–742 (2009). 0908.3948.
43. Kroupa, P., Tout, C. A. & Gilmore, G. The distribution of low-mass stars in the Galactic disc. *Mon. Not. Roy. Astron. Soc.* **262**, 545–587 (1993).
44. Cassan, A. et al. One or more bound planets per Milky Way star from microlensing observations. *Nature* **481**, 167–169 (2012). 1202.0903.
45. Mayor, M. et al. The HARPS search for southern extra-solar planets XXXIV. Occurrence, mass distribution and orbital properties of super-Earths and Neptune-mass planets. *arXiv e-prints* (2011). 1109.2497.
46. Johnson, J. A. et al. A New Planet around an M Dwarf: Revealing a Correlation between Exoplanets and Stellar Mass. *Astrophys. J.* **670**, 833–840 (2007). 0707.2409.
47. Winn, J. N. & Fabrycky, D. C. The Occurrence and Architecture of Exoplanetary Systems. *Annu. Rev. Astron. Astrophys.* **53**, 409–447 (2015). 1410.4199.
48. Suzuki, D. et al. The Exoplanet Mass-ratio Function from the MOA-II Survey: Discovery of a Break and Likely Peak at a Neptune Mass. *Astrophys. J.* **833**, 145 (2016). 1612.03939.
49. Zhang, S. et al. The Disk Substructures at High Angular Resolution Project (DSHARP). VII. The Planet-Disk Interactions Interpretation. *Astrophys. J. Lett.* **869**, L47 (2018). 1812.04045.
50. Izidoro, A., Morbidelli, A., Raymond, S. N., Hersant, F. & Pierens, A. Accretion of Uranus and Neptune from inward-migrating planetary embryos blocked by Jupiter and Saturn. *Astron. Astrophys.* **582**, A99 (2015). 1506.03029.

51. Rafikov, R. R. II/2017 ‘Oumuamua-like Interstellar Asteroids as Possible Messengers from Dead Stars. *Astrophys. J.* **861**, 35 (2018). 1801.02658.
52. Moro-Martín, A. Origin of II/‘Oumuamua. I. An Ejected Protoplanetary Disk Object? *Astrophys. J.* **866**, 131 (2018). 1810.02148.
53. Moro-Martín, A. Origin of II/‘Oumuamua. II. An Ejected Exo-Oort Cloud Object? *Astron. J.* **157**, 86 (2019). 1811.00023.
54. Simon, J. B., Armitage, P. J., Youdin, A. N. & Li, R. Evidence for Universality in the Initial Planetesimal Mass Function. *Astrophys. J. Lett.* **847**, L12 (2017). 1705.03889.
55. Schäfer, U., Yang, C.-C. & Johansen, A. Initial mass function of planetesimals formed by the streaming instability. *Astron. Astrophys.* **597**, A69 (2017). 1611.02285.
56. Dohnanyi, J. S. Collisional Model of Asteroids and Their Debris. *J. Geophys. Res.* **74**, 2531–2554 (1969).
57. Pajola, M. et al. Size-frequency distribution of boulders ≥ 7 m on comet 67P/Churyumov-Gerasimenko. *Astron. Astrophys.* **583**, A37 (2015).
58. Burgasser, A. J. et al. The Brown Dwarf Kinematics Project (BDKP). IV. Radial Velocities of 85 Late-M and L Dwarfs with MagE. *Astrophys. J. Supp. Ser.* **220**, 18 (2015). 1507.00057.
59. Anguiano, B., Majewski, S. R., Freeman, K. C., Mitschang, A. W. & Smith, M. C. The velocity ellipsoid in the Galactic disc using Gaia DR1. *Mon. Not. Roy. Astron. Soc.* **474**, 854–865 (2018). 1710.08479.
60. Portegies Zwart, S., Torres, S., Pelupessy, I., Bédorf, J. & Cai, M. X. The origin of interstellar asteroidal objects like II/2017 U1 ‘Oumuamua. *Mon. Not. Roy. Astron. Soc.* **479**, L17–L22 (2018). 1711.03558.
61. Almeida-Fernandes, F. & Rocha-Pinto, H. J. A kinematical age for the interstellar object II/‘Oumuamua. *Mon. Not. Roy. Astron. Soc.* **480**, 4903–4911 (2018). 1808.03637.
62. Meech, K. J. & Svoren, J. Using cometary activity to trace the physical and chemical evolution of cometary nuclei, *Comets II* (ed. M.C. Festou, H.U. Keller, H.A. Weaver) 317–335 (2004).
63. Pätzold, M. et al. The nucleus of comet 67P/Churyumov-Gerasimenko - Part I: The global view - nucleus mass, mass loss, porosity and implications. *Mon. Not. Roy. Astron. Soc.* (2018).
64. Seligman, D., Laughlin, G. & Batygin, K. On the Anomalous Acceleration of II/2017 U1 ‘Oumuamua. *arXiv e-prints* (2019). 1903.04723.
65. Fernández, Y. R. et al. Physical Properties of the Nucleus of Comet 2P/Encke. *Icarus* **147**, 145–160 (2000).
66. Sekanina, Z. Comet Bowell (1980b) - an active-looking dormant object. *Astron. J.* **87**, 161–169 (1982).
67. Fink, U. Comet Yanaka (1988r) - A new class of carbon-poor comet. *Science* **257**, 1926–1929 (1992).
68. Schleicher, D. G. The Extremely Anomalous Molecular Abundances of Comet 96P/Machholz 1 from Narrowband Photometry. *Astron. J.* **136**, 2204–2213 (2008).
69. A’Hearn, M. F. et al. Cometary Volatiles and the Origin of Comets. *Astrophys. J.* **758**, 29 (2012).
70. Ootsubo, T. et al. AKARI Near-infrared Spectroscopic Survey for CO₂ in 18 Comets. *Astrophys. J.* **752**, 15 (2012).
71. Biver, N. et al. The extraordinary composition of the blue comet C/2016 R2 (PanSTARRS). *Astron. Astrophys.* **619**, A127 (2018). 1809.08086.

72. Seligman, D. & Laughlin, G. The Feasibility and Benefits of In Situ Exploration of 'Oumuamua-like Objects. Astron. J. **155**, 217 (2018). 1803.07022.
73. Rickman, H., Kamel, L., Froeschle, C. & Festou, M. C. Nongravitational effects and the aging of periodic comets. Astron. J. **102**, 1446–1463 (1991).
74. Nesvorný, D. et al. Origin and Evolution of Short-period Comets. Astrophys. J. **845**, 27 (2017). 1706.07447.
75. Micheli, M., Tholen, D. J. & Elliott, G. T. Detection of radiation pressure acting on 2009 BD. New Astronomy **17**, 446–452 (2012). 1106.0564.
76. Sekanina, Z. & Kracht, R. Preperihelion Outbursts and Disintegration of Comet C/2017 S3 (Pan-STARRS). arXiv e-prints (2018). 1812.07054.
77. Moro-Martín, A. Could 1I/'Oumuamua be an Icy Fractal Aggregate? Astrophys. J. Lett. **872**, L32 (2019).
78. Loeb, A. Six Strange Facts About 'Oumuamua. ArXiv e-prints (2018). 1811.08832.
79. Siraj, A. & Loeb, A. 'Oumuamua's Geometry Could Be More Extreme than Previously Inferred. Research Notes of the American Astronomical Society **3**, 15 (2019).
80. Thomas, C. A. et al. ExploreNEOs. V. Average Albedo by Taxonomic Complex in the Near-Earth Asteroid Population. Astron. J. **142**, 85 (2011).
81. Kokotanekova, R. et al. Rotation of cometary nuclei: new light curves and an update of the ensemble properties of Jupiter-family comets. Mon. Not. Roy. Astron. Soc. **471**, 2974–3007 (2017). 1707.02133.
82. Katz, J. I. Why is interstellar object 1I/2017 U1 ('Oumuamua) rocky, tumbling and possibly very prolate? Mon. Not. Roy. Astron. Soc. **478**, L95–L98 (2018). 1802.02273.
83. Rafikov, R. R. Spin Evolution and Cometary Interpretation of the Interstellar Minor Object 1I/2017 'Oumuamua. Astrophys. J. Lett. **867**, L17 (2018). 1809.06389.
84. Čuk, M. 1I/'Oumuamua as a Tidal Disruption Fragment from a Binary Star System. Astrophys. J. Lett. **852**, L15 (2018). 1712.01823.
85. Domokos, G., Sipos, A. Á., Szabó, G. M. & Várkonyi, P. L. Formation of Sharp Edges and Planar Areas of Asteroids by Polyhedral Abrasion. Astrophys. J. Lett. **699**, L13–L16 (2009). 0904.4423.
86. Vavilov, D. E. & Medvedev, Y. D. Dust bombardment can explain the extremely elongated shape of 1I/'Oumuamua and the lack of interstellar objects. Mon. Not. Roy. Astron. Soc. (2019). 1812.11334.
87. Sugiura, K., Kobayashi, H. & Inutsuka, S.-i. Collisional Elongation: Possible Origin of Extremely Elongated Shape of 1I/'Oumuamua. arXiv e-prints (2019). 1903.06373.
88. Stern, S. A. et al. Overview of initial results from the reconnaissance flyby of a Kuiper Belt planetesimal: 2014 MU69. arXiv e-prints arXiv:1901.02578 (2019). 1901.02578.
89. Pravec, P. et al. Tumbling asteroids. Icarus **173**, 108–131 (2005).
90. Kwiecinski, J. A., Krause, A. L. & Van Gorder, R. A. Effects of tidal torques on 1I/2017 U1 ('Oumuamua). Icarus **311**, 170–174 (2018).
91. Zuluaga, J. I., Sánchez-Hernández, O., Sucerquia, M. & Ferrín, I. A General Method for Assessing the Origin of Interstellar Small Bodies: The Case of 1I/2017 U1 ('Oumuamua). Astron. J. **155**, 236 (2018). 1711.09397.
92. Dybczyński, P. A. & Królikowska, M. Investigating the dynamical history of the interstellar object 'Oumuamua. Astron. Astrophys. **610**, L11 (2018). 1711.06618.

93. Zhang, Q. Prospects for Backtracing 1I/'Oumuamua and Future Interstellar Objects. *Astrophys. J. Lett.* **852**, L13 (2018). 1712.08059.
94. Gaidos, E. What and whence 1I/'Oumuamua: a contact binary from the debris of a young planetary system? *Mon. Not. Roy. Astron. Soc.* **477**, 5692–5699 (2018). 1712.06721.
95. Feng, F. & Jones, H. R. A. 'Oumuamua as a Messenger from the Local Association. *Astrophys. J. Lett.* **852**, L27 (2018). 1711.08800.
96. Cook, N. V., Ragozzine, D., Granvik, M. & Stephens, D. C. Realistic Detectability of Close Interstellar Comets. *Astrophys. J.* **825**, 51 (2016). 1607.08162.